Advanced Robotics

ISSN: 0169-1864 (Print) 1568-5535 (Online) Journal homepage: https://www.tandfonline.com/loi/tadr20

A Gaussian process-based RRT planner for the exploration of an unknown and cluttered environment with a UAV

Kwangjin Yang , Seng Keat Gan & Salah Sukkarieh

To cite this article: Kwangjin Yang , Seng Keat Gan & Salah Sukkarieh (2013) A Gaussian process-based RRT planner for the exploration of an unknown and cluttered environment with a UAV, Advanced Robotics, 27:6, 431-443, DOI: 10.1080/01691864.2013.756386

To link to this article: https://doi.org/10.1080/01691864.2013.756386

Advanced Robotics, 2013
Vol. 27, No. 6, 431–443, http://dx.doi.org/10.1080/01691864.2013.756386

Taylor & Francis
Taylor & Francis Group

FULL PAPER

A Gaussian process-based RRT planner for the exploration of an unknown and cluttered environment with a UAV

Kwangjin Yang*, Seng Keat Gan and Salah Sukkarieh

Korea Air Force Academy, P.O. Box 335-2, Ssangsoo Namil 363-849, Cheongwon, Chungbuk, Republic of Korea

(*Received 28 February 2012; accepted 28 April 2012*)

A new framework which adopts a rapidly-exploring random tree (RRT) path planner with a Gaussian process (GP) occupancy map is developed for the navigation and exploration of an unknown but cluttered environment. The GP map outputs the probability of occupancy given any selected query point in the continuous space and thus makes it possible to explore the full space when used in conjunction with a continuous path planner. Furthermore, the GP map-generated path is embedded with the probability of collision along the path which lends itself to obstacle avoidance. Finally, the GP map-building algorithm is extended to include an exploration mission considering the differential constraints of a rotary unmanned aerial vehicle and the limitation arising from the environment. Using mutual information as an information-theoretic measure, an informative path which reduces the uncertainty of the environment is generated. Simulation results show that GP map combined with RRT planner can achieve the 3D navigation and exploration task successfully in unknown and complex environments.

Keywords: Gaussian processes; information-theoretic exploration; map building; rapidly-exploring random tree; unmanned aerial vehicle

1. Introduction

Autonomous navigation in unknown cluttered environments is a challenging problem. To achieve this task the vehicle must have the ability to build an environment representation, generate a safe and feasible path and execute the plan reliably. A path planner plans a path based on its understanding about the environment. In a global collision-free path planning problem, the environment is represented by an occupancy map that contains the joint sensory information about the robot operation space [1]. The most straightforward approach is to discretise the operational area into a pre-defined uniform grid where each grid cell holds the probability of occupancy within the cell [2]. This grid-based path planning approach has been widely used and successfully demonstrated for real-time applications, especially well suited for robots that operate in two-dimensional planar domains [3–5]. However, in three-dimensional applications, the grid-based approach suffers greatly from the curse of dimensionality because the grid density required to reasonably represent the 3D operational environment to a certain resolution exponentially increases. Furthermore, the flexibility of the path planner is restricted by the resolution and orientation of the grid.

We tackle this problem by replacing the traditional grid-based occupancy map approach with a Gaussian Process (GP) occupancy map for path planning. The GP map operates directly on the collected environment data, which eliminate the grid-based map and the concerns with grid size, grid shape, obstacle shape and map resolution. There is no need to associate the data to discrete cells and thus no information is lost. The GP map outputs the probability of occupancy given any selected query point in the continuous space. This grants it the potential to explore all possible paths in the full space when used in conjunction with a continuous path planner. Furthermore, a path planned with a GP map is embedded with the probability of collision along the path. This valuable information is not available in other grid- or graph-based frameworks.

In this paper, a rapidly-exploring random tree (RRT) path planner is used for the planning algorithm. The first application of the GP map combined with RRT path planner is to generate a collision-free path from an initial state to a goal state. The GP map is well matched with the RRT framework since it works as collision detection module that implicitly represents free space. The RRT expands its network as part of the exploration mission to get information of the unknown cluttered environment.

*Corresponding author. Email: ykj4957@gmail.com, kyang@afa.ac.kr

Autonomous vehicles with sensing capabilities can actively take advantage of their mobility to get information about the environment. A key component of active environment sensing systems is the dependence of information gathering on robot motion, and the ability to predict in advance the effect of robot motion on the quality of information that is collected [6]. Information-theoretic approaches, which use information measures, such as entropy, Fisher information and mutual information as an objective functionality, have been actively investigated [7–10]. In this paper, appropriate selection of the information criteria is important because each information measure has a different way of characterising the uncertainty. Mutual information is used as an information measure because it provides a pre-observation measure of the usefulness of obtaining information about the value of the sensor measurement [11].

The role of the planner in the exploration mission is to generate a path that maximises the information of the environment. Therefore, it is important to evaluate properly the uncertainty of the environment based on the accumulated environment data, because the quality of path is quantified by this evaluation. GP is an excellent method to evaluate the uncertainty because it has an inference capability in occluded areas. The exploration problem, which aims to minimise the uncertainty in the environment, is similar to the sensor management problem. The main difference between mobile robotic networks and sensor management is that there is no restriction to the deployment of sensors in sensor networks [12,13], but there are severe constraints in a mobile robot such as a unmanned aerial vehicle (UAV): kinematic and dynamic constraints which restrict the evolution of the vehicle states. In addition to the differential constraint of the vehicle, there are other constraints which make the exploration task challenging. The observation is also constrained by the limited sensor field of view, and the difficulties are compounded by the occlusion due to obstacles. Finally, the vehicle must satisfy the safety condition which ensures no collision with obstacles. All of these constraints complicate the planning problem. This paper proposes an information-theoretic path planning algorithm for the exploration mission which takes into account these constraints within the RRT framework.

The rest of the paper is organised as follows: Section 2 presents a brief background of the GP and how it can be used as a tool to generate a continuous occupancy map. Section 3 outlines the RRT path planning algorithm considering non-holonomic constraints and its adaptive path replanning strategy. Section 4 addresses information-theoretic exploration in cluttered environments. Section 5 presents simulation results of a UAV performing a navigation and exploration task, and the conclusions are presented thereafter.

2. 3D GP occupancy map

2.1. Foundations of GPs

GPs are a powerful non-parametric tools for regression based on locally available data-sets. It represents a family of distributions over functions and inference takes place directly in the function space [14]. It is particularly useful to infer the most likely function value f_* and its corresponding variance for a given test input $\mathbf{x}_*$ when exact observation on $\mathbf{x}_*$ is not available. Especially for the case when there is no information about the underlying function, inference with GP can be achieved by placing a multivariate Gaussian distribution across the function space.

Consider $\chi = \{(\mathbf{x}_i, y_i) | i = 1, ..., n\}$ as a collection of N data-sets, where $\mathbf{x}_i \in \mathbb{R}^D$ represents a D dimensional training input and $y_i \in \mathbb{R}$, the corresponding scalar training output (in our case, y_i is $+1$ or -1 for occupied and non-occupied, respectively). Condition on χ, for any selected testing input $\mathbf{x}_*$, the predictive distribution of the function output becomes

$$f_* \mid \mathbf{x}_*, \chi \sim N(\mu_*, \sigma_*^2) \tag{1}$$

with mean

$$\mu_* = k(\mathbf{x}_*, \mathbf{x})[k(\mathbf{x}, \mathbf{x}) + \sigma_n^2 I]^{-1}\mathbf{y} \tag{2}$$

and variance

$$\sigma_*^2 = k(\mathbf{x}_*, \mathbf{x}_*) - k(\mathbf{x}_*, \mathbf{x})\left[k(\mathbf{x}, \mathbf{x}) + \sigma_n^2 I\right]^{-1} k(\mathbf{x}, \mathbf{x}_*) \tag{3}$$

Here, $k(\mathbf{x}, \mathbf{x}')$ is the GP covariance or kernel function, which effectively sets the correlation between the output of $\mathbf{x}$ and $\mathbf{x}'$ based on trained kernel hyperparameters.

Selection of the appropriate covariance function highly depends on the application. A commonly used kernel is the stationary squared-exponential (SE) kernel:

$$k(\mathbf{x}, \mathbf{x}') = \sigma_f^2 \exp\left(-\frac{1}{2}(\mathbf{x} - \mathbf{x}')^T \mathbf{M}(\mathbf{x} - \mathbf{x}')\right) \tag{4}$$

where σ_f^2 is the signal strength, σ_n^2 the Gaussian noise variance and $\mathbf{M} = \mathrm{diag}[1/l_1^2, ..., 1/l_D^2]$, where l_i is the length scale that sets the kernel smoothness characteristic in different dimensions. There exist other covariance functions that outperform SE in terms of modelling non-continuous spatial functions, such as the neural-network demonstrated in [15]. Nevertheless, the SE is by far the most computationally efficient kernel that suits our application.

2.2. Probabilistic least square classification (PLSC)

Our aim here is to estimate the probability of collision for any chosen location in 3D workspace for collision-free path planning. There are various classification algorithms available, but, as described by [14] and implemented by

[15], one simple, yet, efficient method is to treat the classification as a GP regression problem and then further squash the GP predictions through a cumulative Gaussian sigmoid function to obtain a valid probability

$$p(y_i|\mathbf{x}, y_{-i}, \theta) = \Phi\left(\frac{y_i(\alpha\mu_i + \beta)}{\sqrt{1 + \alpha^2\sigma_i^2}}\right) \quad (5)$$

where y_{-i} is all training data except the point $(\mathbf{x}_i, y_i)$, Φ is a cumulative unit Gaussian which is defined as $\Phi = (2\pi)^{-1/2}\int_{-\infty}^{z}\exp(-t^2/2)\,dt$, θ denotes the hyperparameters of the covariance function, α and β are the classifier hyperparameters that can be trained using the leave-one-out (LOO) cross-validation procedure as described in Section 2.4. The full method is called PLSC.

2.3. 3D laser sensor model

We consider a rotary UAV (RUAV). It is assumed that the RUAV platform is equipped with a sparse 3D laser range finder, capable of scanning n_b beams every instant the sensor is activated, as depicted in Figure 1. Each time the sensor scans the environment, the following information is stored for each beam segment $\Lambda^k = \{(s_i, \mathbf{u}_i, b_i)|i = 1{:}\ n_b\}^k$ where s_i, $\mathbf{u}_i$ and b_i are, respectively, the sensor position, beam vector from sensor to return position and a boolean indicating either 1 if the beam hits an obstacle and 0 otherwise.

2.4. Training GP and classifier hyperparameters

Training data-sets can be obtained by firstly flying the RUAV platform around an obstacle in a simulated environment, like one in Figure 1(a), collecting laser beam data. The collected laser beam segments are then divided into discrete points where each point is described by its 3D location $\mathbf{x}$ and corresponding label y, used for the hyperparameter training described below.

Training the GP hyperparameters is effectively setting the appropriate properties for the covariance function. A common method is based on maximisation of the log of the marginal likelihood:

$$\theta_{opt} = \arg\max[\ln p(\mathbf{y}|\mathbf{x}, \theta)] \quad (6)$$

where

$$\ln p(\mathbf{y}|\mathbf{x}, \theta) = -\frac{1}{2}\mathbf{y}^T K_y \mathbf{y} - \frac{1}{2}\ln|K_y| - \frac{n}{2}\ln 2\pi \quad (7)$$

and $K_y = k(\mathbf{x}, \mathbf{x}) + \sigma_n^2 I$. The optimal solution of this method produces a model that balances between model complexity and data fitness, which is known as the Occam's razor principle.

Having trained the GP hyperparameters, the classifier hyperparameters can then be trained using the cross-validation approach, based on maximising the sum of the log LOO probability:

$$\{\alpha, \beta\}_{opt} = \arg\max\left[\sum_{i=1}^{N}\ln p(y_i|\mathbf{x}, \mathbf{y}_{-i}, \theta, \alpha, \beta)\right] \quad (8)$$

where

$$\ln p(y_i|\mathbf{x}, \mathbf{y}_{-i}, \theta) = -\frac{1}{2}\ln\sigma_i^2 - \frac{(y_i - \mu_i)^2}{2\sigma_i^2} - \frac{1}{2}\ln 2\pi \quad (9)$$

and

$$\mu_i|\theta = \mathbf{y}_i - [k(\mathbf{x}, \mathbf{x})^{-1}y]_i / [k(\mathbf{x}, \mathbf{x})^{-1}]_{ii} \quad (10)$$

$$\sigma_i^2|\theta = 1/\left[k(\mathbf{x}, \mathbf{x})^{-1}\right]_{ii} \quad (11)$$

are the mean and variance after leaving out the training data-set y_i. Note that these hyperparameters are fixed once they are trained in this application.

2.5. Sparse training data extraction

Λ is a database of collected continuous beam segments representing the true occupancy information about the environment. When the occupancy hypothesis of a point $\mathbf{x}_*$ is queried, a series of sparse spatial training data is to be extracted from its local neighbourhood database subset $\Lambda_{\mathbf{x}_*} = \{\Lambda_{j,\mathbf{x}_*}|\, j = 1 : n_s\}$ where n_s is the number of the nearest beam segment. Amongst $\Lambda_{\mathbf{x}_*}$, training input $\mathbf{x}$ and its corresponding label $\mathbf{y}$ can thus be extracted using Algorithm 2. Lines 1 and 2 determine the distance L and location of the point that is projected orthogonally from $\mathbf{x}_*$ onto the beam segment $\mathbf{u}$ (note that $\hat{\mathbf{u}}$ is the unit vector of $\mathbf{u}$). Line 3 extracts the end of the beam segment. Lines 4 to 10 simply infer the conditions when the point $\mathbf{x}_\perp$ lies outside of the beam segment. Lines 11 to 13 use a simple logic to set a safety boundary around obstacles for our path planning purpose that will be further described in the following section.

Algorithm 1. Sparse training data extraction.
Require : $\Lambda_{\mathbf{x}_*}, \mathbf{x}_*$
1: $L \leftarrow \mathbf{a} \cdot \hat{\mathbf{u}}$
2: $x_\perp \leftarrow \mathbf{s} + L\,\hat{\mathbf{u}}$
3: $\mathbf{x}_{end} \leftarrow \mathbf{s} + \mathbf{u}$
4: **if** $d \leqslant 0$ **then**
5: $\quad \mathbf{x} \leftarrow \mathbf{s},\ y \leftarrow -1$
6: **else if** $d \geqslant |\mathbf{u}|$**then**
7: $\quad \mathbf{x} \leftarrow \mathbf{x}_{end},\ y \leftarrow 2b - 1$
8: **else**
9: $\quad \mathbf{x} \leftarrow \mathbf{x}_\perp,\ y \leftarrow -1$
10: **end if**
11: **if** $b = 1\ \ |\mathbf{x}_{end} - \mathbf{x}_*| \leqslant d_{\text{safety}}$ **then**
12: $\quad \mathbf{x} \leftarrow \mathbf{x}_*\ ,\ y \leftarrow 1$
13: **end if**

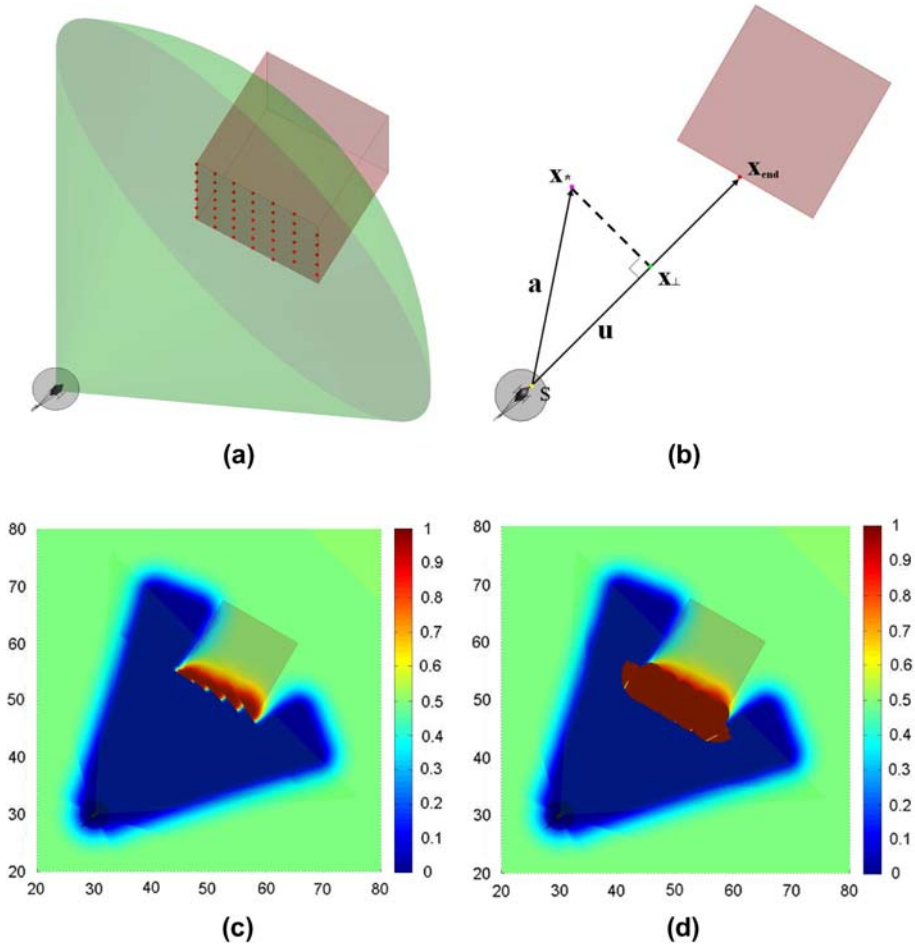

Figure 1. GP occupancy map construction: (a) shows the instant where an obstacle is detected within the FOV of the 3D laser range finder. The notation used in Algorithm 1 for extracting training data from a single laser beam is illustrated in (b). Diagram (c) illustrates the high-resolution horizontal plane GP map at the height of the sensor with the colour indicating the probability of obstacle. The modifications made to suit path planning are shown in (d) where a safety boundary parameter d_{safety} of 5 m is used. Note that (c) and (d) are for visualisation purposes. There is no need to construct the full map for online path planning applications.

2.6. *Safety boundary construction*

Setting a safety region around obstacles is crucial for an airborne platform as flying close to obstacles significantly increases the risk of collision. A simple yet efficient way is to include this feature in the GP map framework, appearing in lines 11 to 13 in Algorithm 1.

The aim is to enforce maximum correlation between the output of $\mathbf{x}_{end}$ and $\mathbf{x}_*$, for $\mathbf{x}_{end}$ that is extracted from an obstacle beam, when the distance between them is less than the safety distance d_{safety}. The simplest way to achieve this without modifying the GP framework is to simply set $\mathbf{x}$ to be the same as $\mathbf{x}_*$, which, referring to Equation (4), effectively sets $k(\mathbf{x}, \mathbf{x}')$ to the maximum value of the covariance function. This method directly embeds the safety boundary feature in the training dataset extraction process, flexibly controlled by the single parameter d_{safety} with no induced cost while transitioning from 2D to 3D workspace.

3. Path planning using GP occupancy map

This section describes the path planning algorithm which takes into account differential constraints of the vehicle and then addresses replanning strategies based on probability of collision along the path produced by the GP map.

3.1. *RRT path planning under differential constraints*

RRT is firstly suggested in [16] as an alternative to complete path planning in high degree of freedom configurations and its popularity has significantly increased since then. The RRT algorithm incrementally builds a tree online from the starting point to the goal point by adding a new vertex towards randomly selected points. Having said that, this means that any point in the full continuous space has the potential of being selected by the planner as part of the path, which is in a perfect match to the GP map property for being able to test occupancy condition for any selected location in continuous space.

The holonomic RRT can add any point to the tree if there are no collisions between the node in the tree and the candidate random point. In this work, however, a node can only be added to the tree if it satisfies the feasibility condition arising from the differential constraints.

Figure 2(a) shows a path smoothing algorithm to generate a continuous curvature path satisfying an upper bound curvature constraint which is suggested in [17,18]. In that work, the path smoothing algorithm was applied only after the RRT planner generates a path. This decoupled approach cannot guarantee the generation of a feasible path. In this research, the path smoothing algorithm is incorporated to the RRT planner, thus it always satisfies the maximum curvature constraints of the system.

The two variables to generate an upper bounded continuous curvature path in Figure 2(a) are d and β which are determined as [18]

$$d = \frac{c_4 \cdot \sin\beta}{\kappa_{\max} \cdot \cos^2\beta}, \quad \beta = \frac{\gamma}{2} \tag{12}$$

where $\kappa_{\max}$ denotes the maximum curvature and

$$c_1 = 7.2364, c_2 = \frac{2}{5}\left(\sqrt{6}-1\right), c_3 = \frac{c_2+4}{c_1+6}, c_4 = \frac{(c_2+4)^2}{54c_3}$$

The maximum curvature ($\kappa_{\max}$) is specified based on the kinematic constraints of the vehicle, thus γ is the unique variable for checking feasibility. Once γ is decided, the length of tree d is obtained using Equation (12).

Figure 2(b) illustrates 100 candidate paths with different tree depths. Here, the maximum curvature is set as $\kappa_{\max} = 0.1$ and $\gamma = 0.3\pi$, which results in $d = 6.42$ from Equation (12). Regardless of the tree depths, the path generated by RRT planner satisfies both the curvature continuity and the maximum curvature constraints as shown in Figure 2(c).

3.2. *Adaptive dynamic replanning*

The main requirement in the planning process is the ability to perform collision checks. Given a path, the grid-based methods discretise the path into n points, associate these points to their nearest grid cell and decide if a point is collision-free based on the status in that cell. The process is similar in the GP map approach, but instead of associating points into cells, the query points are directly passed into the GP map collision checker that extract corresponding sparse training data, apply GP regression, transform into valid probabilities which are classified as collision or non-collision based on a user defined threshold.

A GP map-generated path shows the probability of collision along the path, depicted by the coloured path in Figure 3. This information can be applicable to the other system modules. For example, a guidance module can implement this into a reactive platform speed controller, travelling faster along path segments with a low probability of collision. Also, a perception module can implement this information to perform active sensing decisions, reactively changing the sensor orientation to scan areas of low information. Here, we employ it as an indicator for path replanning.

Figure 3 shows the change in path probability of collision before and after sensing an obstacle. The colour bar on the right represents the probability of collision. If there is no information about the environment, the probability of collision is 0.5, which is represented by the green colour. If there is no collision, the probability of collision approaches zero, which is represented by the

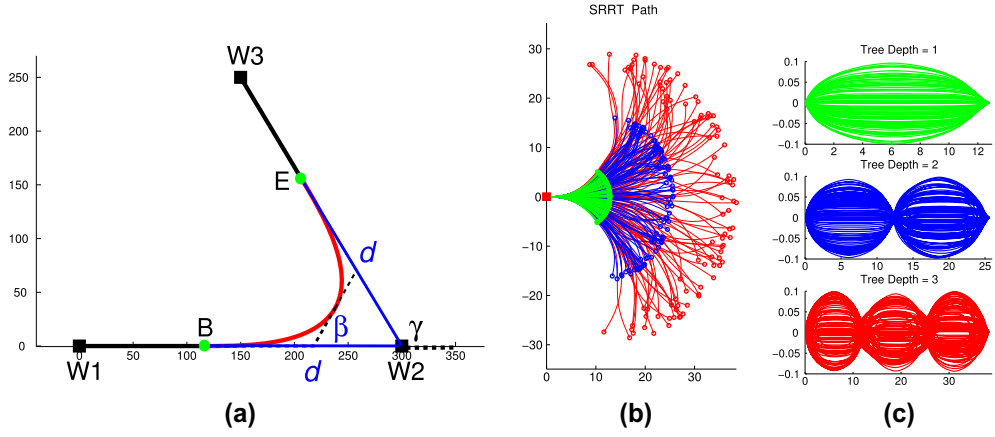

Figure 2. Smooth paths generated by RRT and their curvatures: (a) upper bounded continuous curvature path smoothing algorithm: Upper bounded continuous curvature path are determined once the maximum curvature ($\kappa_{\max}$) and β are specified. (b) and (c) show 100 candidate paths and curvatures with different tree depths. Green paths are for tree depth of one, blue paths are tree depth two and red paths are tree depth three.

blue colour. If collision is detected along the path, the probability of collision approaches one, which is represented by the red colour. The probability of collision is depicted by the colour on the path and its value is updated with new perceptual information as shown in Figure 3(a). Once collision is detected along the path by the circle, replanning is triggered to form a new collision-free path as shown in Figure 3(b). Note that this new path penetrates through the obstacle as the laser beams have only detected the front side of the obstacle.

4. Information-theoretic path planning for exploration mission

In the previous section, the GP is used for map building of the environment and this map information is used to generate a collision-free path. In this Section, the application of the GP map is extended not only for collision check but also for evaluation of the information.

4.1. Information measures

The objective of path planning for an exploration mission is to compute a path towards the most informative area. In order to judge the quality of the path, it is necessary to establish the notion of *informativeness*. There are several information measures and each class of information measure results in a different output. The existence of different information measures naturally raises the question of deciding upon the most appropriate measure.

The Fisher information is a useful information measure for Gaussian representations because it is simply the information matrix. However, it is not scalar, and so cannot be used explicitly for preference ordering of posteriors as a measure of information gain [19]. Shannon information is a good measure for making a decision on which observations are the most uncertain. Though Shannon information is a proper measure to evaluate the absolute amount of information, it cannot capture the objective of the exploration task. What is important in the exploration mission is the amount of uncertainty reduction after the observation is made instead of the absolute magnitude of the information itself. Mutual information provides an average measure of how much more information can be obtained if the observations are made. Most importantly, mutual information provides a pre-observation measure of the usefulness of obtaining information through an observation [11]. In that sense, mutual information is a more useful measure than Shannon information. The mutual information is chosen as a measure of evaluation of the information.

4.2. Evaluation of uncertainty of the environment

Consider Λ is a database of collected continuous beam segments. When a point $\mathbf{x}_*$ is queried for the evaluation of information at this point, a series of sparse spatial training data are to be extracted from its local neighbourhood database subset $\Lambda_{\mathbf{x}_*} = \{\Lambda_{j,\mathbf{x}_*} | \, j = 1{:}\, n\}$, where n is the number of the nearest beam segment. Using the *Sparse Training Data Extraction* algorithm in Section 2, n number of orthogonal points are obtained from $\Lambda_{\mathbf{x}_*}$. Let $\mathcal{X} = \{\mathbf{x}_1, \mathbf{x}_2, \ldots, \mathbf{x}_n\}$ be the extracted orthogonal points. Then the covariance at this testing point $\mathbf{x}_*$ is calculated using Equation (13) which comes from Equation (3):

$$\sigma_*^2 = k(\mathbf{x}_*, \mathbf{x}_*) - k(\mathbf{x}_*, \mathbf{x}) k(\mathbf{x}, \mathbf{x})^{-1} k(\mathbf{x}, \mathbf{x}_*) \qquad (13)$$

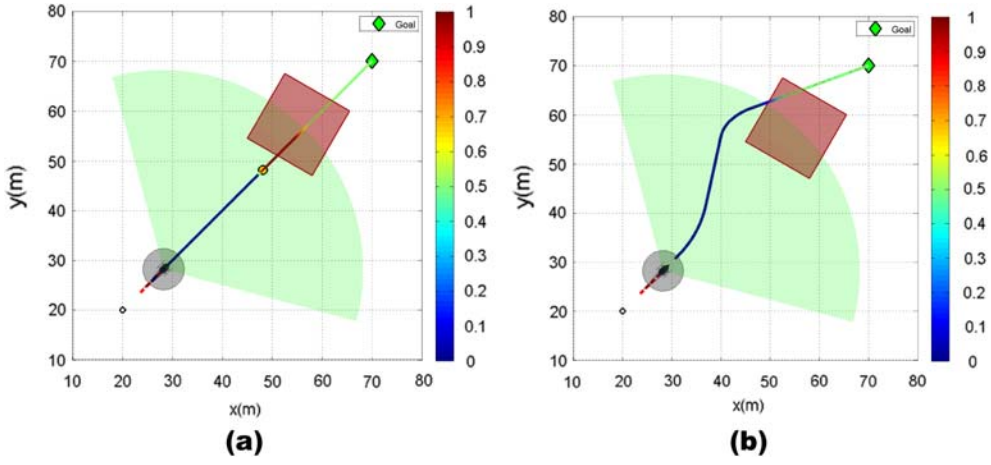

Figure 3. Adaptive path replanning. The probability of collision is depicted by the colour on the path and its value is updated with new perceptual information as shown in (a). Once collision is detected along the path by the circle, replanning is triggered to form a new collision-free path as shown in (b).

Figure 4 shows the laser beam data and the covariance map of the environment. Blue rays in Figure 4(a) show laser beam data ($\mathcal{X} = \{\mathbf{x}_1, \mathbf{x}_2, \cdots, \mathbf{x}_n\}$), and red circles represent laser beam hit locations on obstacles, and squares are obstacles. The environment is discretised to evaluate the covariance map of the environment. The purpose of this discretisation is only intended for visualisation of the covariance. In practice, this discretisation is not required. The result of the covariance evaluation of the environment is shown in Figure 4(b).

The advantage of GP is that it has an ability to infer into an area occluded by obstacles. Figure 4(b) shows this property. Purple denotes a highly uncertain area and blue denotes a certain area; the colour between purple and blue denotes the level of inference of uncertainty. If there is laser beam data surrounding a testing point, the GP function generates a small covariance value which is represented as a blue colour. However, if there is no laser beam data around a testing point, it outputs a high covariance value which is represented as a purple colour. Though there is no laser beam data near the testing point, the GP can infer the uncertainty based on neighbouring laser beam data. The ability to extract information from an unexplored area is the strength of the GP.

4.3. Information-theoretic path planning algorithm

The objective of exploration is to get as much information as possible on the environment in a cost-effective way. Generating an informative path satisfying both the feasibility requirements of the differential constraints and the safety condition is difficult. In this research, the RRT algorithm in Section 3 is used to generate a path satisfying the feasibility and safety conditions and the GP in Section 2 is utilised to incorporate information measures for the evaluation of the path.

Algorithm 2. Information-theoretic path planning algorithm
1: Candidate path generation
2: Sensor emulation
3: Information evaluation
4: Informative path selection

Algorithm 2 shows the proposed information-theoretic path planning algorithm. There are four functions in this algorithm. First, the candidate path generation function generates several candidate paths as shown in Figure 5. Second, the sensor emulation function simulates laser beams along the path. Thirdly, the information evaluation function calculates the mutual information of each path. Finally, the informative path selection function compares the information gain of each path and chooses the most informative path.

4.3.1. Candidate path generation

The role of the candidate path generation function is to generate several candidate paths which satisfy the feasibility and safety conditions using GP map.

Figure 6 shows the generated paths at the current vehicle position in Figure 4(a). All paths satisfy the nonholonomic constraints of the vehicle. There are no collisions between obstacles near the starting point but there are collisions where there is little information about the environment. When a path is planned, the uncertain area is regarded as free space. If the uncertain area is considered an obstacle, the planner cannot generate a path outside of the certain area. This assumption does not affect the safety of the vehicle because as the vehicle receives information about the environment, the obstacles are identified. If any potential collisions are detected along the path, the planner triggers replanning of the path to generate a new collision-free path.

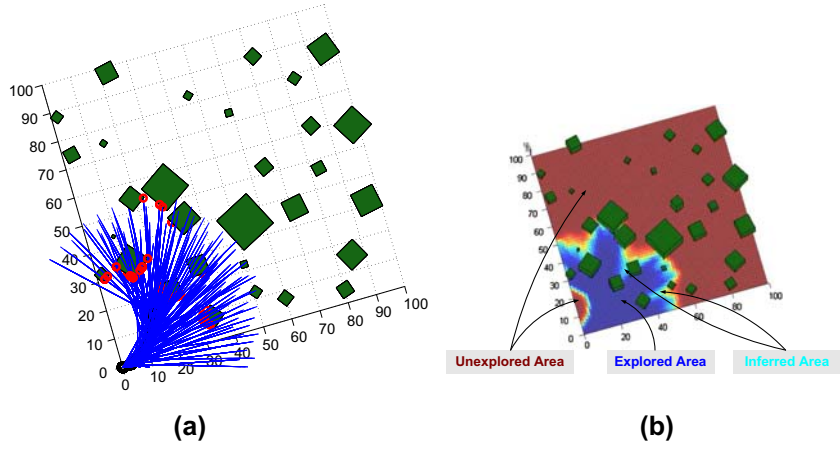

Figure 4. Laser beam data and covariance map: Blue rays in (a) show laser beam data and red circles represent laser beam hit locations with obstacles. (b) shows the covariance map of the environment based on the laser beam data collected by the vehicle. The uncertainty of the occluded area is smaller than the unexplored area though there is no laser beam data behind obstacles.

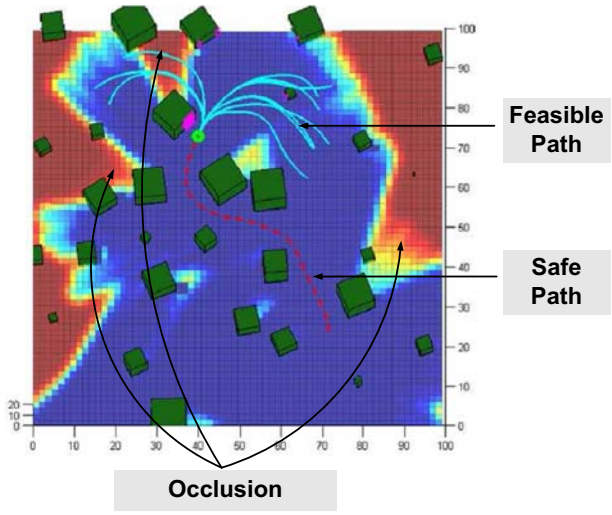

Figure 5. The difficulties of an exploration mission: the planner must satisfy the differential constraints of the vehicle, and generate a collision-free path, overcoming a limited sensor field of view and occlusion due to obstacles.

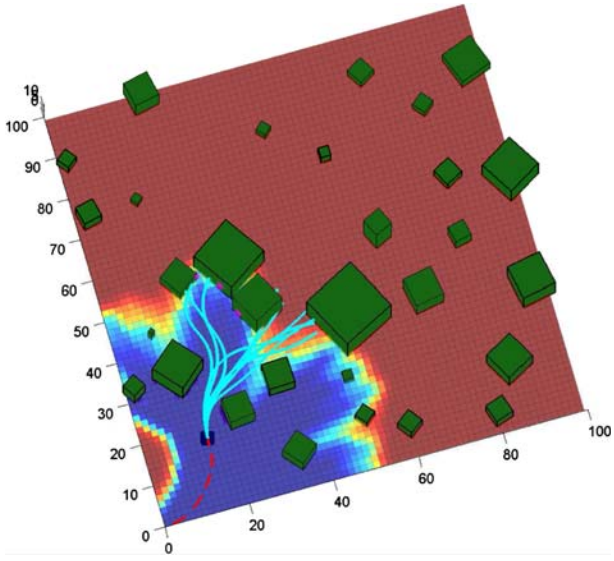

Figure 6. Candidate path generation satisfying the feasibility requirement and safety condition: the square is a starting point of the planning, the red dashed line is the flight path of the vehicle and the cyan curves are generated candidate paths.

4.3.2. Sensor emulation

To evaluate the information of the path, it is necessary to emulate the laser beam along the path. Firstly, the sensor emulation points are decided and then laser beam data are radiated at these points.

Figure 7 shows the laser beam data. Blue rays in Figure 7(a) represent accumulated real laser beam data (Λ^r), red rays in Figure 7(b) represent simulated laser beam data (Λ^s) and Λ^c represents combined blue and red laser beams in Figure 7(b). Figure 7(c) and (d) are 2D representations of Figure 7(a) and (b).

4.3.3. Information evaluation

The quality of the path can be determined by measuring the amount of reduction in the uncertainty of the environment. The goal of information evaluation is to select a path with the least uncertainty after observations are made. Mutual information is the fittest measure to quantify the variance of information about the un-sensed area. Mutual information can be obtained by comparing the covariance of the environment using the real accumulated laser data with the combined laser data.

Consider Λ^r as the accumulated real laser beam data, Λ^s as the simulated laser beam data at points obtained from the *Sensor Emulation* algorithm and $\Lambda^c = \Lambda^r \cup \Lambda^s$ as the combined data of both laser beams. There are N testing points $\mathcal{X}^t = \{\mathbf{x}_1^t, \mathbf{x}_2^t, \cdots, \mathbf{x}_N^t\}$ in the environment for the evaluation of the information.

Using the *Sparse Training Data Extraction* algorithm in Section 2, n number of orthogonal points are obtained. Let $\mathcal{X}^r = \{\mathbf{x}_1^r, \mathbf{x}_2^r, \cdots, \mathbf{x}_n^r\}$ be the extracted orthogonal points from accumulated real laser beam data (Λ_r), and $\mathcal{X}_i^c = \{\mathbf{x}_1^c, \mathbf{x}_2^c, \cdots, \mathbf{x}_n^c\}$ be the extracted orthogonal points from i_{th} combined laser beam data (Λ_i^c).

Condition on $\mathcal{X}^r$ and $\mathcal{X}_i^c$, the covariance at testing input $\mathcal{X}^t$ becomes

$$\mathbf{K}^r = k(\mathbf{x}^t, \mathbf{x}^t) - k(\mathbf{x}^t, \mathbf{x}^r)k(\mathbf{x}^r, \mathbf{x}^r)^{-1}k(\mathbf{x}^r, \mathbf{x}^t) \tag{14}$$

$$\mathbf{K}_i^c = k(\mathbf{x}^t, \mathbf{x}^t) - k(\mathbf{x}^t, \mathbf{x}^c)k(\mathbf{x}^c, \mathbf{x}^c)^{-1}k(\mathbf{x}^c, \mathbf{x}^t) \tag{15}$$

where $\mathbf{K}^r$ is a covariance obtained from accumulated real laser beam data and $\mathbf{K}_i^c$ is a predicted covariance of ith path.

Then, the mutual information in ith candidate path can be obtained:

$$I_i = \log|\mathbf{K}^r| - \log|\mathbf{K}_i^c| \tag{16}$$

where $\log|\mathbf{K}^r|$ is an entropy of the environment before sensor observation and $\log|\mathbf{K}_i^c|$ is an entropy of the environment after sensor observation of ith path. is made.

4.3.4. Informative path selection

Mutual information explicitly presents the amount of the uncertainty reduction. Therefore, a path which outputs maximum mutual information can offer more information about the environment. After evaluating the mutual information of all candidate paths, a path which gets the largest mutual information is chosen as the most informative path.

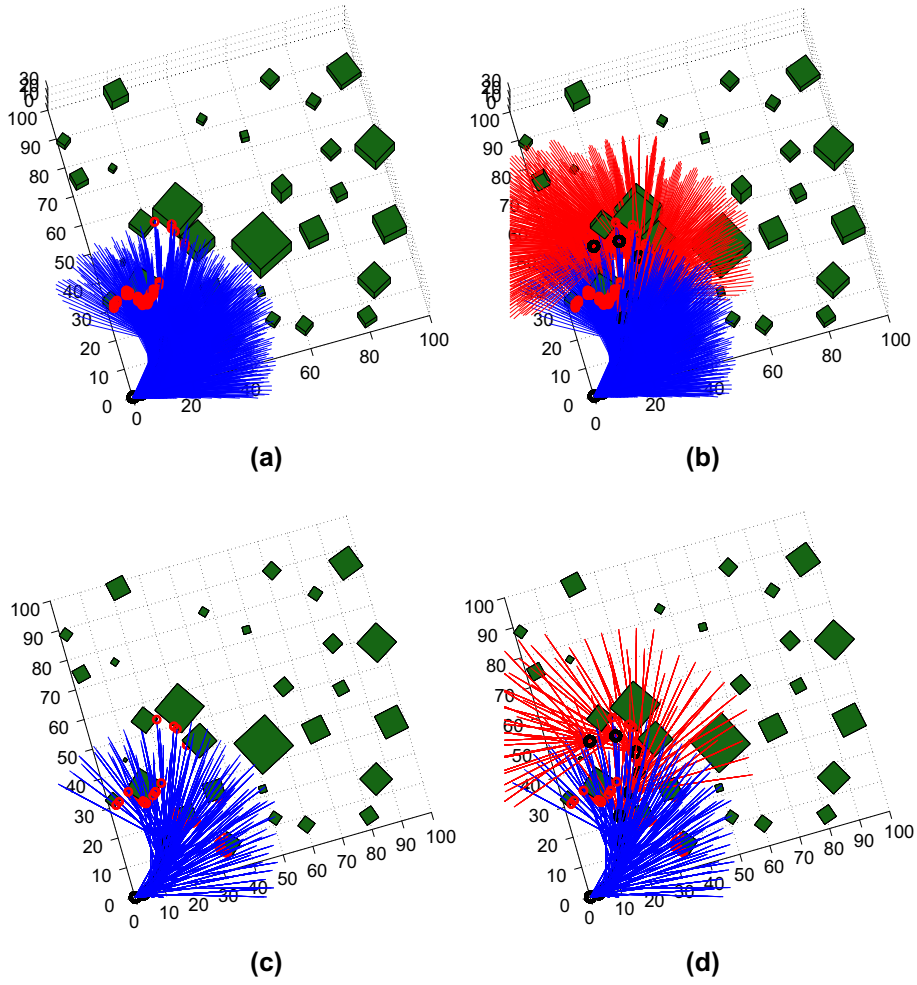

Figure 7. Laser beam data: (a) shows 3D accumulated real laser beam data. (b) red rays represent simulated laser beam data. (c) and (d) are the 2D representations of the laser beams of (a) and (b).

5. Simulation experiments

In this section, the simulation experiments are conducted to investigate the navigation and exploration performance of the proposed algorithm. An RUAV is used as a platform to perform these missions and model predictive control method is used as a controller to track the path. The detailed descriptions of the dynamic model of RUAV and path tracking controller are shown in [20]. The first simulation is done in 3D urban-like environment to investigate the planning property using the GP map. The second simulation is conducted in a cluttered 3D natural environment to test the feasibility of the GP map to complex planning problems. Finally, an exploration mission in unknown cluttered environment is implemented to examine the information-theoretic exploration performance.

5.1. 3D path planning in urban environment

A first simulation is conducted which performs online path planning in an urban-like environment. The RUAV starts at the origin with no prior information about the environment and the goal is located at [100,100,0]. It is operating at 5 m/s constant speed with a fixed 3D laser sensor operating at 1 Hz, maximum range of 40 m and a field of view of 180° in both pan and tilt directions (hemisphere). The obstacles are simulated as cubic blocks. The colour bar corresponds to the probability of collision. A classification threshold of 0.6 is set to distinguish between the possible planning region and the obstacles region. Probabilities above this threshold are classified as obstacle, depicted by the non-uniform boundaries around the detected obstacles.

Figure 8 illustrates six snapshots of path replanning after the sensor detects obstacles along the path ahead of the vehicle. The RUAV traversed path is shown in red (not related to colour bar) whilst the planned path ahead of the UAV is portrayed with the probability of collision along the path. The green hemisphere represents the field of view of the laser sensor and the green asterisks on obstacles represent the laser hits to obstacles.

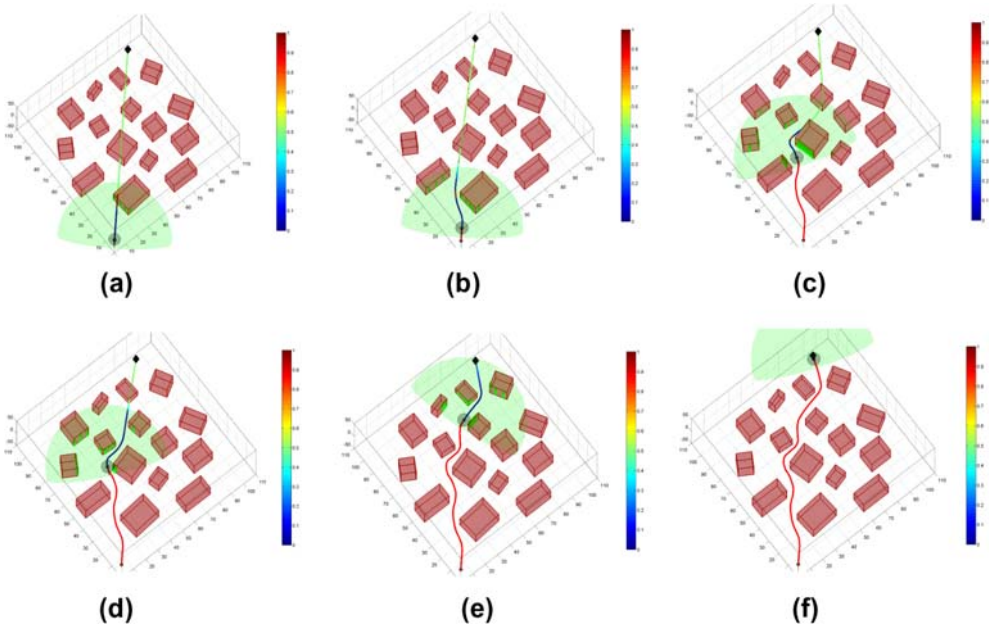

Figure 8. Path planning in urban environment: the RUAV starts at the origin with no prior information about the environment. By gradually building a map about the environment using the GP, the RUAV can achieve autonomous navigation in an unknown cluttered urban environment.

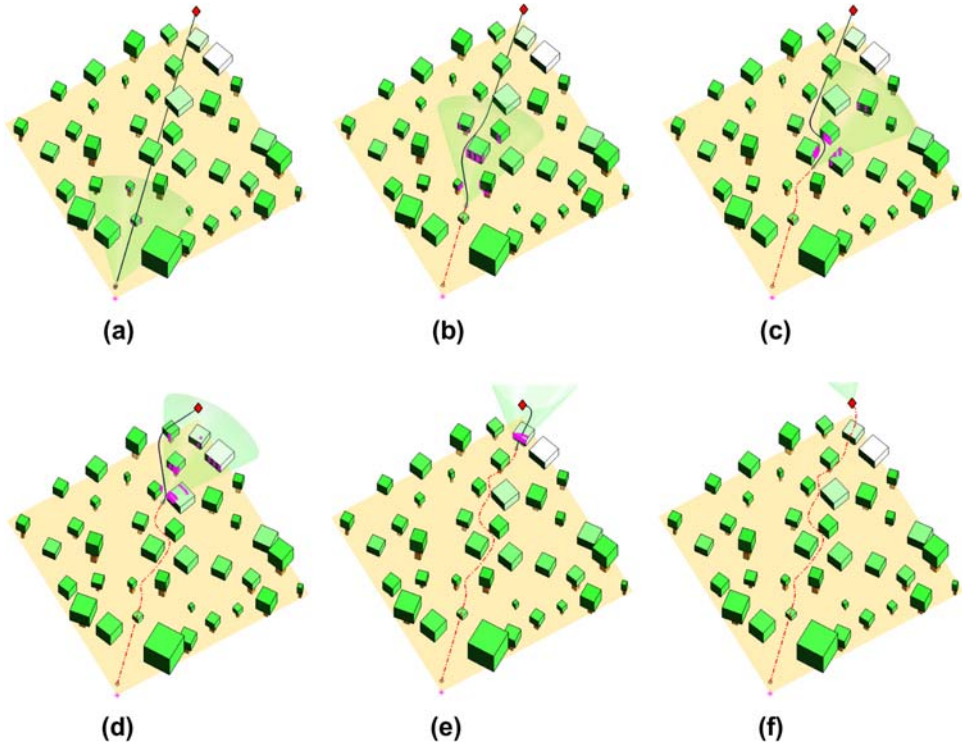

Figure 9. Path planning in a cluttered natural environment: the field of view of the laser sensor is reduced to 60 degrees to investigate the planning ability in more difficult conditions. The planner replans the path more often than in the urban environment case because the natural environment is more complex.

Figure 8(a) shows the initial path which is generated without any prior information about the environment. The reference path is a straight line which connects the starting point to the goal point. Figure 8(b) shows the

first path replanning. The obstacle in front of the RUAV is identified and the RRT planner generates a new safe path. It should be noted that the planned path goes through the obstacle in Figure 8(c) though the path is within the sensor field of view. This is because the laser beams have only detected the right side of the obstacle but cannot detect the north side of the obstacle. Therefore, the planner recognises the north side of the obstacle as a free space, which results in the penetration of the obstacle. However, the planner generates a collision-free path after obtaining the information of this obstacle, as shown in Figure 8(d). Figure 8(e) and (f) illustrate the successive path planning stages until the goal point is reached. By gradually building a map about the environment using the GP, the RUAV can achieve autonomous navigation in an unknown cluttered urban environment. From Figure 8, it can be clearly seen that the probability of collisions along the path after replanning always stays below the 0.6 threshold, as expected.

5.2. 3D path planning in a cluttered natural environment

The second simulation is conducted in a complex natural environment. The RUAV is operating at 5 m/s constant speed with a fixed 3D laser sensor operating at 1 Hz, maximum range of 40 m. However, the field of view of the laser sensor is reduced from 180 to 60° to investigate the planning ability in more difficult natural conditions around trees. The trunks are simulated as brown cubic blocks and the branches and leaves are simulated as a green cubic blocks. The colour bar is not represented in this simulation.

Figure 9 illustrates snapshots of path replanning in the cluttered natural environment. The RUAV-traversed

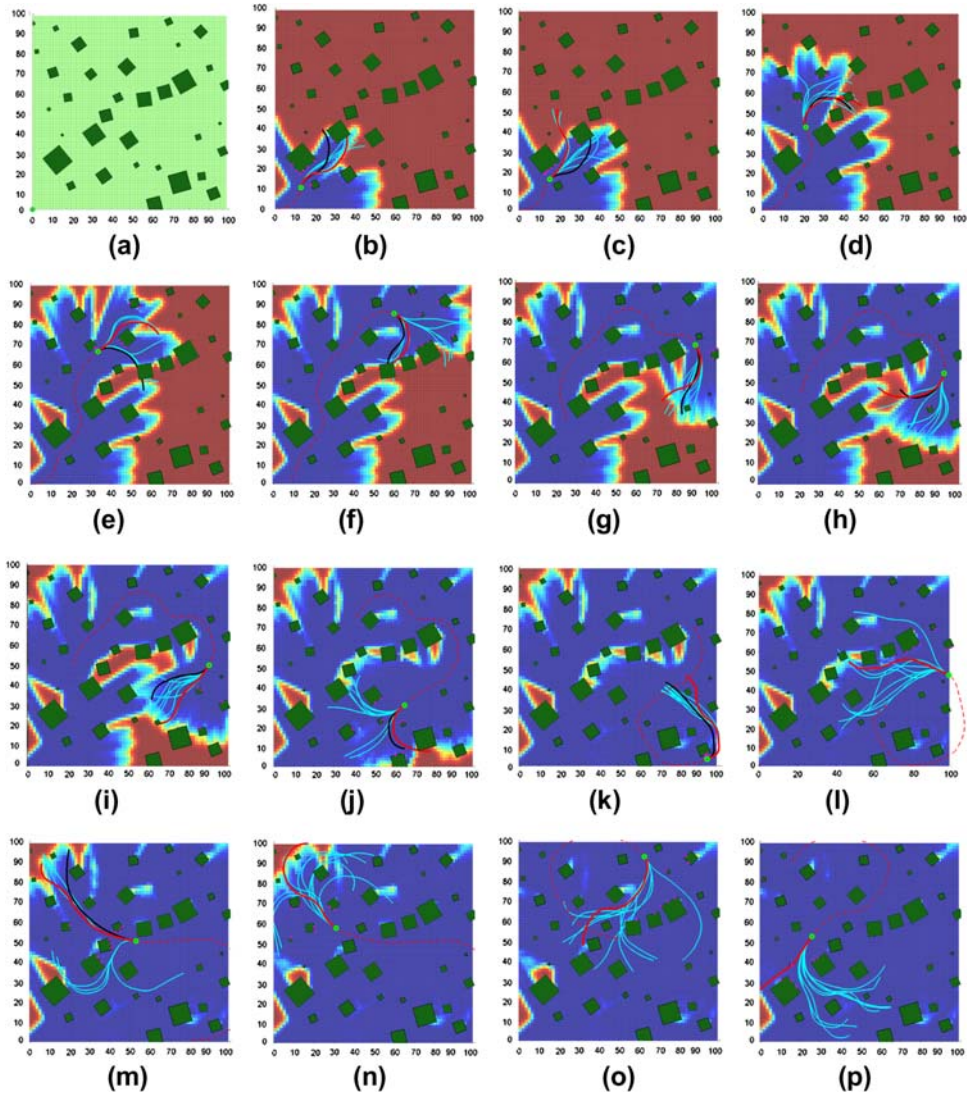

Figure 10. Information-theoretic exploration in unknown cluttered environment: there are severe occlusions due to obstacles but the GP can infer the information about these areas and achieve the exploration mission successfully.

path is shown in red dash-dot line and the planned path ahead of the UAV is represented by the black line. The green corn represents the field of view of the laser sensor and the magenta asterisks on obstacles represent the laser hits to obstacles.

Figure 9(a) shows the initial path which is a straight line connecting the starting point to the goal point. Figure 9(b) presents the first path replanning. The RUAV goes over the small tree because it is located below the altitude at which the RUAV is flying. Figure 9(c)–(f) illustrates the successive path planning stages. The planner replans the path more often than in the urban environment case because the natural environment is more complex. From Figure 9, it can be seen that the RUAV completes the autonomous navigation mission in the complex natural environment successfully.

5.3. Information-theoretic exploration in unknown environment

From the previous two simulations, it can be seen that the RUAV can achieve the navigation mission successfully regardless of the complexity of the environment. The third simulation is conducted of an exploration mission. The objective of exploration is to maximise information about the environment. The environment is filled with 30 obstacles of which the locations and size are randomly generated. Figure 10(a) shows the environment to explore. Initially, the planner has no information about the environment. Figure 10(b) shows 10 candidate paths and a covariance map of the environment. Purple denotes highly uncertain areas and the blue denotes certain areas; the colour between the purple and blue denotes the level of inference of uncertainty. The magenta asterisks represent laser beam hits to obstacles. The red curve denotes the selected best informative path, the black curve is the previous best path, the cyan curves represent the other candidate paths and the dotted red line is the flight path of the RUAV. There are severe occlusions due to obstacles but the GP can infer the information about these areas even though there are no laser beam data within the occluded area. Figure 10 shows the progress of the exploration mission. As can be expected, the mutual information measure selects the most informative path which maximally reduces the uncertainty of the environment. Figure 10(p) shows that the planner generates a path toward the left-bottom corner of the environment because this area is the most uncertain region in the environment.

6. Conclusions

An information-theoretic path planning for exploration in unknown cluttered environments is proposed. Instead of using traditional grid-based occupancy maps, a GP model is used to build an environmental map. The GP map performs inference directly on the collected sensor data-sets which allows it to infer the probability of collision and uncertainty for any query point in continuous 3D space, removing the need for maintaining a full discrete map. This GP map is fused with the RRT path planner to plan a safe path and acquire information about the environment. Simulation results show that a 3D navigation and exploration tasks with GP map in unknown complex environment are achieved successfully. In our future work, we would like to implement data management techniques to maintain the computational efficiency of our method with the increasing data-set. Furthermore, we would like to utilise non-linear non-stationary covariance functions that could potentially infer the underlying structures and patterns of the environment. Such covariance functions would require GP training in real-time which is challenging with large data-set.

Notes on contributors

Kwangjin Yang received the BS degree from Republic of Korea Air-Force Academy, Korea, in 1996, and the MS degree from Pohang University of Science and Technology (POSTECH), Korea, in 2002 both in mechanical engineering, and the Ph.D. degree from University of Sydney, Australia, in 2010 in Aerospace engineering. He is currently an associate professor in the Department of Aerospace and Mechanical Engineering, Korea Air-Force Academy. His research interests include unmanned aerial vehicle, mobile robot navigation, path planning and cooperative search and track.

Seng Keat Gan received the BE degree in Aeronautical (Space) Engineering in 2008 and completed his Ph.D in aerospace robotics in 2012, both from the University of Sydney. He is currently a research associate at the Australian Centre for Field Robotics (ACFR) at the University of Sydney. His research focuses on multi-agent systems coordination for information gathering, path planning and collision avoidance.

Salah Sukkarieh is the professor of Robotics and Intelligent Systems at the University of Sydney and the research director for the Australian Centre for Field Robotics. He received Honours in BE Mechatronics Engineering in 1997 and completed his Ph.D. in aerospace robotics in 2000 at the University of Sydney. He has been the principal research and development lead for many of the autonomous projects at the ACFR including automation of straddle carriers for port operations; unmanned air vehicle research with the US Air Force, BAE systems and for environmental monitoring; and

ground vehicle automation for various defence and mining organisations. He is in various international robotics panels and committees and has given over 70 talks to international industry and research organisations.

References

[1] Scherer S, Singh S, Chamberlain L, Elgersma M. Flying fast and low among obstacles: methodology and experiments. Int. J. Rob. Res. 2008;27:549–574.

[2] LaValle SM. Planning algorithms. Cambridge: Cambridge University Press; 2006.

[3] Ferguson D, Stentz A. Using interpolation to improve path planning: the Field D* algorithm. J. Field Rob. 2006;23:79–101.

[4] Grabowski R, Weatherly R, Bolling R, Seidel D, Shadid M, Jones A. MITRE meteor: an off-road autonomous vehicle for DARPA's grand challenge. J. Field Rob. 2006;23:811–835.

[5] Montemerlo M, Becker J, Bhat S, Dahlkamp H, Dolgov D, Thrun S. Junior: the stanford entry in the urban challenge. J. Field Rob. 2008;25:569–597.

[6] Frew EW. Cooperative standoff tracking of uncertain moving targets using active robot networks. IIEEE International Conference on Robotics and Automation; 2007 Apr; Roma, Italy.

[7] Bourgault F, Makarenko AA, Williams SB, Grocholsky B, H. Durrant-Whyte H. Information based adaptive robotic exploration. IEEE/RSJ International Conference on Intelligent Robots and Systems; 2002 Oct; Lausanne, Switzerland.

[8] Stachnissy C, Grisettiyz G, Burgard W. Information gain-based exploration Using Rao-Blackwellized particle filters. Cambridge (MA): Robotics: Science and Systems; 2005.

[9] Ryan AD, Durrant-Whyte H, Hedrick JK. Information-theoretic sensor motion control for distributed estimation. Seattle: International Mechanical Engineering Congress and Exposition; 2007.

[10] Frew EW. Information-theoretic integration of sensing and communication for active robot networks. Athens: International conference on Robot communication and coordination; 2007.

[11] Grocholsky B. Information-theoretic control of multiple sensor platforms [PhD thesis]. Sydney: The University of Sydney; 2002.

[12] Singh A, Ramos F, Durrant-Whyte H, Kaiser W. Modeling and decision making in spatio-temporal process for environmental surveillance. Anchorage: IIEEE International Conference on Robotics and Automation; 2010.

[13] Krause A, Singh A, Guestrin C. Near-optimal sensor placements in Gaussian processes: theory, efficient algorithms and empirical studies. J. Mach. Learn. Res. 2008;9:235–284.

[14] Rasmussen C, Williams C. Gaussian processes for machine learning. Cambridge: MIT; 2006.

[15] Callaghan SO, Ramos FT, Durrant-Whyte H. Contextual occupancy maps using gaussian processes. IIEEE International Conference on Robotics and Automation; 2009; Kobe, Japan.

[16] LaValle SM. Rapidly-exploring random trees: a new tool for path planning TR 98–11. Ames, IA: Computer Science Dept, Iowa State University; 1998.

[17] Yang K, Sukkarieh S. 3D smooth path planning for a UAV in cluttered natural environments. IEEE/RSJ International Conference on Intelligent Robots and Systems; 2008 Sep; Nice, France.

[18] Yang K, Sukkarieh S. An analytical continuous-curvature path-smoothing algorithm. IEEE Transactions on Robotics 2010;26:561–568.

[19] Cole DT. A cooperative UAS architecture for information-theoretic search and track [PhD thesis]. Sydney: The University of Sydney; 2009.

[20] Yang K, Gan S, Sukkarieh S. An efficient path planning and control algorithm for RUAV's in unknown and cluttered environments. Journal of Intelligent and Robotic Systems 2010;57:101–122.